

Establishment of a Novel Cell Line for the Enhanced Production of Recombinant Adeno-Associated Virus Vectors for Gene Therapy

Stifani Satkunanathan, Jun Wheeler, Robin Thorpe, and Yuan Zhao

Abstract

Adeno-associated viral (AAV) vectors show great promise because of their excellent safety profile; however, pre-existing immune responses have necessitated the administration of high titer AAV, posing a significant challenge to the advancement of gene therapy involving AAV vectors. Recombinant AAV vectors contain minimum viral proteins necessary for their assembly and gene delivery functions. During the process of AAV assembly and production, AAV vectors acquire, inherently and submissively, various cellular proteins, but the identity of these proteins is poorly characterized. We reason that by identifying host cell proteins inherently associated with AAV vectors we may better understand the contribution of cellular components to AAV vector assembly and, ultimately, may improve the production of AAV vectors for gene therapy. In this study, three serotypes of recombinant AAV, namely AAV2, AAV5, and AAV8, were investigated. We used liquid chromatography-mass spectrometry/mass spectrometry (LC-MS/MS) methods to identify protein composition in purified AAV vectors, confirmed protein identities using western blotting, and explored the potential function of selected proteins in AAV vector production using small hairpin (shRNA) methods. Using LC-MS/MS, we identified 44 AAV-associated cellular proteins including Y-box binding protein (YB1). We showed for the first time that the establishment of a novel producer cell line by introducing an shRNA sequence down-regulating YB1 resulted in up to 45- and 9-fold increase in physical vector genome titers of AAV2 and AAV8, respectively, and up to 7-fold increase in AAV2 transduction vector genome titers. Our results revealed that YB1 gene knockdown promoted AAV2 *rep* expression and vector DNA production and reduced the number of empty particles in AAV2 products, suggesting that YB1 plays an important role in AAV vector assembly by competition with adenovirus E2A and AAV capsid proteins for binding to the inverted terminal repeat (ITR) sequence. The significance and implications of our findings in future improvement of AAV production are discussed.

Introduction

ADENO-ASSOCIATED VIRAL (AAV) VECTORS have an excellent safety profile because wild-type AAV has never been associated with any human disease and is thus a popular, and by far the most successful, vector used for gene therapies. AAV vectors have been extensively studied in clinical trials, for example, for haemophilia B (Nathwani *et al.*, 2011), heart disease (Jessup *et al.*, 2011), and congenital blindness (Bennett *et al.*, 2012). In addition, the first EU-licensed gene therapy product, Glybera, for the treatment of a rare metabolic disease (Bryant *et al.*, 2013) is based on AAV, exemplifying a great promise for AAV vectors in gene therapy. Despite many advances in AAV vector design, barriers such

as a pre-existing immune response have necessitated the administration of high titer AAV and, in many cases, a combined administration of an immune-suppressant to achieve clinical efficacy, presenting a significant challenge in AAV production and considerable safety implications in the clinical use of AAV vectors.

AAV vectors are most commonly produced by a transient cotransfection of AAV plasmids and a helper plasmid derived from another virus, for example, an adenovirus. Significant progress has recently been made in large-scale production and robust purification of AAV to support clinical development (Brument *et al.*, 2002; Davidoff *et al.*, 2004; Shiau *et al.*, 2005; Okada *et al.*, 2009; Lock *et al.*, 2012). However, production of high-titer AAV is still a significant challenge,

as in the case of the first marketed product Glybera, which is required to be administered to patients as a dose of 3×10^{12} vg/kg via 40 or 60 multiple injections (Bryant *et al.*, 2013). To improve AAV production, in terms of high-titer and better quality production of AAV vectors, significant efforts have been made, including the generation of partial stable producer cell lines with the integration of AAV plasmids to allow a two-step and controlled production process (Gao *et al.*, 1998; Martin *et al.*, 2013) and the reduction of immunoreactivity of AAV vectors (Wu, 2001; Kaludov *et al.*, 2002; Davidoff *et al.*, 2004; Qu *et al.*, 2007).

Factors, either cellular or viral, that contribute to the AAV vector production are still largely unknown. In general, viruses package their genomes into protein capsids either via association of structural proteins with the viral genome or insertion of viral genomes into preassembled capsids. AAV viruses have adopted the latter process (Myers and Carter, 1980; King *et al.*, 2001); however, the actual mechanism by which viral DNA is inserted into capsids remains unknown. It has been reported that specific amino acid interactions are required for efficient insertion of viral DNA and a single amino acid mutation or gross conformation change of AAV capsid proteins results in deficiency of packaging of the viral genome (Bleker *et al.*, 2006; DiPrimio *et al.*, 2008; Gerlach *et al.*, 2011). There have been very limited studies on the involvement of cellular proteins in AAV assembly. The life cycle of AAV strongly depends on helper virus function provided by adenovirus, herpes virus, or papillomavirus families (Muzyczka, 1992; Nicolas *et al.*, 2012).

In addition to the direct helper function, the helper virus may also induce entry of host cell into S-phase and lead to changes of cellular milieu, which are necessary for AAV assembly (Carter, 2004). Genotoxic or cytotoxic factors such as SV40 large T antigen (LTAg) that transformed or altered a cell cycle have also been shown to support AAV replication and assembly (Nicolas *et al.*, 2012). It has been reported that total HeLa cell proteins and DNA helicase are required for AAV assembly (Steinbach *et al.*, 1997; King *et al.*, 2001; Sonntag *et al.*, 2011; Naumer *et al.*, 2012). A recent report using proteomics analysis of AAV vectors showed the association of 10 cellular proteins, for example, Nucleolin (NCL) and nucleophosmin (NPM1), with AAV vectors (Dong *et al.*, 2014). NCL and NPM1 are nucleolus proteins with many functions, which bind to AAV2 capsids and shuttle the AAV proteins between the cytoplasm and nucleus (Qiu and Brown, 1999; Bevington *et al.*, 2007; Johnson and Samulski, 2009), demonstrating an important role of cellular proteins in AAV capsid assembly or vector genome encapsidation.

We reason that by analyzing host cellular proteins coproduced and copurified with AAV vectors, we may identify differences in protein composition among the three AAV serotypes AAV2, AAV5, and AAV8; better understand the role of cellular proteins in AAV assembly; and ultimately improve AAV vector production. For this, three serotypes of AAV vectors were produced using transient transfection and were purified using affinity chromatography to allow and simplify component analysis. The purified samples were further subjected to liquid chromatography-mass spectrometry/mass spectrometry (LC-MS/MS) analysis, and some of MS data were confirmed using immunoblotting. Potential function of the selected proteins Annexin A5 and YB1 were further investigated using shRNA methods.

Our study revealed for the first time an important role of Y-box binding protein 1 (YB1) in AAV vector production. Introducing the short hairpin (shRNA) sequence Y4 that targets and down-regulates the YB1 gene to AAV producer cells resulted in up to 45- and 9-fold increase in physical vector genome titers of AAV2 and AAV8, respectively, and up to 7-fold increase in AAV2 infectious vector genome titers. The significance of our findings should be considered in the context of future development of production methods for AAV-based gene therapy products. This study may also provide insight into the control of AAV morphogenesis.

Materials and Methods

Vector production

Three AAV serotypes, that is, AAV2, AAV5, and AAV8, were produced and studied. AAV particles were expressed from three plasmids—pHelper (Stratagene), pAAV-RC encoding AAV Rep-Cap, and pAAV-hrGFP (Stratagene). Plasmid pAAV2/2 Rep-Cap was purchased from Stratagene, and plasmids pAAV5-RC and pAAV2/8-RC were kindly provided by Professor J. Chiorini (National Institute of Dental and Craniofacial Research) and Professor James Wilson (University of Pennsylvania), respectively. All vectors were produced by transient transfection of human embryonic kidney 293T cells (Stratagene) using the calcium phosphate-transfection method (Chen and Okayama, 1988). Vector producer cells were harvested, subjected to five cycles of freeze thaw to release vector particles, and cellular debris was removed by centrifugation (2000 g). The supernatant containing vector particles was then filtered through 0.45 μ m filters (Millipore) and diluted with 20 mM bis-tris propane buffer prior to chromatography (Davidoff *et al.*, 2004).

Affinity chromatography

A Gilson HPLC system (Anachem) was used for chromatography, which was equipped with a UV-detector (Gilson, 119), pump (Gilson 306), autosampler (Gilson 231XL), and fraction collector (Gilson FC203B) both fitted with temperature controlled racks connected to a refrigerated recirculating water bath (Grant, SLS), which also cooled the water-jacketed column. The system was controlled using Gilson Unipoint software. An XK 16/26 column (Amersham) was packed to contain a bed volume of 5 ml AVB Sepharose High Performance medium (GE Healthcare), and used following the manufacturer's protocol. Purified vector particles were pooled and dialyzed to equilibrate into phosphate-buffered saline (PBS) in a 10K MWCO Slide-A-Lyzer dialysis cassette (Thermo scientific) and concentrated to 1/20 of initial volume using Ultra 5K MWCO centrifugal filter devices (Millipore) before being subjected to vector quantitation.

Total protein was measured using a Pierce BCA protein assay kit (Thermo scientific) and following the manufacturer's protocol. The identity and the predicted amount of capsid proteins were visualized using a SilverXpress staining kit (Invitrogen) according to the manufacturer's protocol.

LC-MS/MS analysis

Purified and concentrated vector samples were digested with trypsin in the presence of 1% Rapigest and 50 mM ammonium bicarbonate (ABC) pH 8.5 for 3 h at 37°C. The

digestion was then terminated by adding HCl before the samples were subjected to MS analysis.

LC-MS/MS was carried out using a mass spectrometry system (Thermo Fisher) equipped with a nano-electrospray ion source and two mass detectors, that is, linear trap (LTQ) and orbitrap, coupled with an Ultimate 3000 nano-LC system, comprising a solvent degasser, a loading pump, a nano-pump, and a thermostated autosampler. After an automated injection, the extracted peptides from each digestion were desalted in a trapping cartridge (PepMap reverse phase C18, 5 μ m 100 Å, 300 μ id \times 5 mm length) (Thermo Fisher) and eluted onto a C18 reversed phase nano-column (3 μ m, 100Å, 5 cm length) (Thermo Fisher) and followed by a 60 min separation under a column flow rate of 0.3 μ L/min using a linear gradient from 5–70% acetonitrile and 0.1% formic acid. After a first survey MS scan (from m/z 400–2000) in the LTQ, the five most intense ions were sequentially isolated and passed to the orbitrap for accurate mass measurement with the resolution of 30,000 parts per million (ppm). These were then fragmented in the linear ion trap at collision-induced energy of 35%. The total cycle time was approximately 30 milliseconds. Data was collected in data-dependent MS/MS mode with dynamic exclusion set to two counts.

Data analysis including mass spectra processing and database searching was carried out using Thermo Proteome Discoverer 1.2 with built-in Sequest. Initial mass tolerances for protein identification by MS were set to 10 ppm. Up to two missed tryptic cleavages were considered and methionine oxidation was set as dynamic modification. Peptide sequences by MS/MS were only included when Xcorrelation scores were greater than 1.5, 2, or 2.2 for charge states 1, 2, and 3, respectively. An unambiguous identification was considered when at least two peptides matched to the protein. The protein FASTA databases were downloaded from www.uniprot.org, release 2012-07, including the complete entries from homo sapiens (taxon identifier 9606) bos taurus (9913); complete genome of AAV2, AAV5, and AAV8; and green fluorescent protein (GFP; P42212).

Treatment of purified vectors with proteinase K

To further evaluate whether cellular protein YB1 was incorporated into AAV particles, purified vectors were treated briefly for 10 min with 10 μ g/mL of proteinase K to digest trace un-incorporated cellular proteins (Denard *et al.*, 2009) followed by adding with proteinase inhibitors to a final concentration of 2 mM, heating 10 min at 90°C before being subjected to immunoblotting.

Immunocytochemistry

Sodiumdodecyl sulfate (SDS)-polyacrylamide gels (10% total acrylamide) were used to resolve protein samples and were subjected to immunoblotting. Samples for immunoblotting were electrophoresed and electroblotted to Hybond enhanced chemiluminescence (ECL) membranes (Amersham). The following primary antibodies were used: mouse anti-AAV2 Rep (Fitzgerald) and AAV5 Cap (Abcam), anti-Annexin A5 (Abcam), anti-CypA (Abnova), anti-RuvB2 (Abcam), anti-hnRNP K (Abcam), anti-YB1 (Abcam), and anti-GAPDH (Abcam). The immunoblots were further incubated with goat anti-mouse, anti-rabbit, or rabbit anti-goat horseradish peroxidase conjugates (Sigma). The immunore-

active proteins were detected using ECL reagents (Amersham). The level of gene knockdown was evaluated using 10 μ g total proteins from shRNA virus-transduced cells following the immunoblotting method as described above. AAV2 capsid proteins were quantified using an ELISA kit and following manufacturer's protocol (Progene) and presented as capsid/mL according to the manufacturer's standard curve conversion.

shRNA interference and the establishment of gene knockdown cell lines

Ten shRNA sequences were used for gene knockdown of Annexin A5 and YB1 and were expressed from plasmid pLKO.1-puro (Sigma) using a lentiviral expression system. The shRNA and lentiviral vector packaging plasmids were transfected into 293T cells using the CaCl₂ transfection method. Control cells were transfected with empty capsids without an shRNA sequence (mock) or a scramble shRNA sequence targeting nonmammalian gene sequences (scramble).

Gene knockdown cell lines were established by transducing parental 293T cells with lentiviral vector (LV)-shRNA vectors, and were then subjected to puromycin selection 48 h after transduction and maintained in culture with the presence of 3 μ g/mL puromycin throughout the study.

Sample preparation for transduction vector genome titration

AAV vectors produced from control, scramble, or gene-knockdown cells were used to transduce HeLa cells (ATCC) overnight. Considering the potential that results from low multiplicity of infection (MOI)-treated samples might be out of a quantitative polymerase chain reaction (qPCR) detection limit and that the results from high MOI samples might reach plateau without giving a linear corresponding range to the viruses used due to limiting factors, for example, receptor completion, we used three MOIs ranging from 10 to 100 to 1000 based on physical genome titers to transduce HeLa cells. Total DNA was extracted from transduced cells using Wizard[®] DNA purification kit (Promega) before being subjected to quantitation of housekeeping gene actin for sample normalization and the determination of AAV transduction genome titers, using qPCR as described in the following section. The transduction titer for each sample was determined based on qPCR results that were obtained from the lowest of the three MOIs used and that were within qPCR detection limit and a linear data range.

Vector preparation for AAV genome titration

Crude or purified AAV vectors were treated with 50 units/mL benzenase (Sigma) at 37°C for 30 min followed by incubation with 50 units/mL DNase I (Invitrogen) at 37°C for 1 h to remove residual plasmid DNA in vector samples. After the inactivation of DNase I at 65°C for 10 min, Proteinase K (20 μ g/mL, Sigma) was then added and incubated at 50°C for 2 h to release vector DNA from AAV capsids followed by inactivation at 95°C for 20 min and before being subjected to qPCR analysis. Cytoplasmic DNA extraction was the same as vector DNA except without Proteinase K digestion of capsid proteins. Genomic DNA was extracted using Wizard[®] DNA Genomic purification kit (Promega).

DNA quantitation using qPCR

AAV physical and transduction vector genome titers were determined by q-PCR with primers and probes targeting cytomegalovirus (CMV) promoters, that is, CMV primers: 5' TTC CTA CTT GGC AGT ACA TCT ACG 3' and 5' GTC AAT GGG GTG GAG ACT TGG 3' and CMV probe: 5' 6FAM-TGA GTC AAA CCG CTA TCC ACG CCC A-TAMRA 3'. Housekeeping genes were quantified by qPCR with actin primers: 5' TGGACTTCGAGCAAGAGATG 3' and 5' GAAGGAAGGCTGGAAGAGTG 3' and probe: 5'(6FAM)CGGCTGCTTCCAGCTCCTCC(TAM) 3'. The plasmid DNA pAAV-hrGFP (Stratagene) and pGEM-actin (in house) were used as reference standards in 10-fold serial dilutions ranging from 10^2 to 10^8 copies. qPCR was carried out using a LightCycler480 (Roche) under the condition of one 10-min cycle at 95°C, followed by 45 cycles of 15 s at 95°C, 30 s at 60°C, and 5 s at 72°C.

Results

Vector Purification

The AAV vectors used in this study were based on three different serotypes, that is, AAV2, AAV5, and AAV8. The AVB Sepharose affinity chromatography used in this study was designed for the purification of adeno-associated viruses. Figure 1a shows a typical protein separation using a 5 ml column containing AVB Sepharose coupled with AAV antibodies and that the majority of proteins were not bound

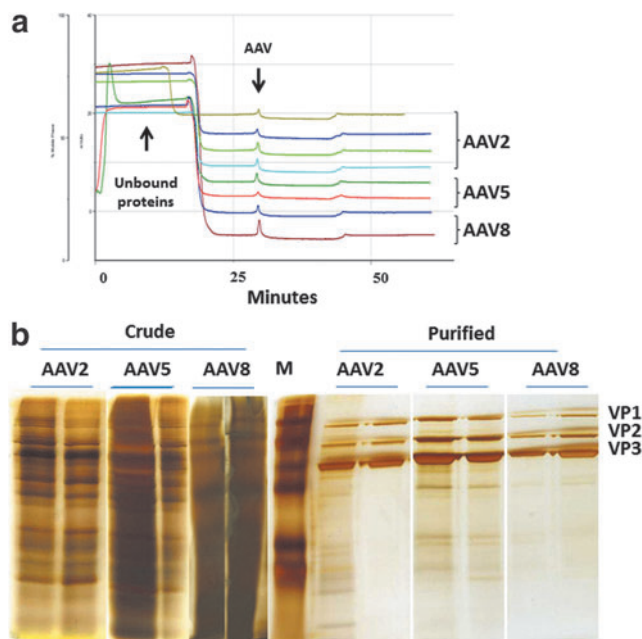


FIG. 1. Protein profile of three serotypes of adeno-associated virus (AAV) vectors before and after AVB Sepharose affinity chromatography. **(a)** A typical chromatography profile, showing the separation of vectors from unbound cellular proteins of independent batches of vectors for three AAV serotypes; and **(b)** the protein profile of silver stained SDS-PAGE gels showing the purity of two batches of AAV vectors before (crude) and after (purified) chromatography, as well as AAV capsid proteins VP1, VP2, and VP3. M, molecular weight markers. Color images available online at www.liebertpub.com/hum

to AAV antibodies and thus flowed through the column before the elution buffer (50 mM glycine, pH 2.7) was applied (Fig. 1a). AAV vectors were eluted at 25–35 min of migration time (Fig. 1a); the protein profile of eluted samples was then visualized using SDS-PAGE and silver staining (Fig. 1b), showing significant purity of AAV samples after chromatography. As expected, three dominant AAV capsid proteins VP1 (81 kDa), VP2 (72 kDa), and VP3 (62 kDa) were evident. Crude, unpurified AAV samples showed many protein bands.

Protein identification using LC-MS/MS

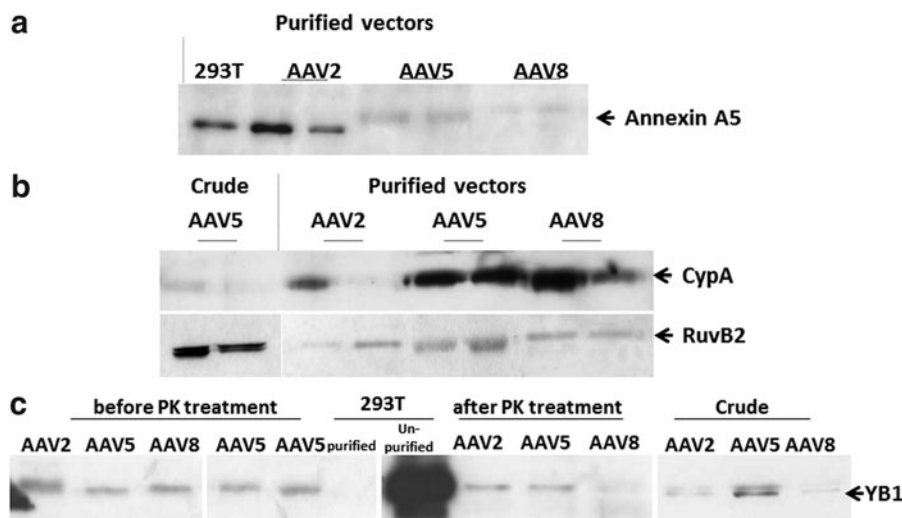
Equal amounts of total proteins from three different types of purified AAV vector samples, that is, AAV2-GFP, AAV5-GFP, and AAV8-GFP were subjected to LC-MS/MS analysis. To minimize data variation, three batches of samples were prepared for each type of vector, with each batch pooled from 40 tissue culture plates (150 mm diameter). Three MS runs were performed for each batch of samples. Our results showed that 44 proteins were detected in at least 2/3 runs of three batches of samples and were thus considered to be significant components and further studied. Among the significant proteins (Supplementary Table S1; Supplementary Data are available online at www.liebertpub.com/hum), 10 proteins were common to 3 serotypes of AAV vectors, including 70 kDa protein 1A/1B, alpha-enolase, GapDH, heat shock, histone H2A type 1H, histone H2B, nucleolin, nucleophosmin, RuvB2, and YB1. Out of eight proteins shared by two serotypes, five proteins were shared by AAV2 and AAV5, indicating a relative similarity between AAV2 and AAV5 vectors. Twenty-six proteins were unique to individual serotypes of vectors.

Confirmation of MS data

To validate MS data, immunoblotting was carried out on five LC-MS/MS identified proteins, that is, Annexin A5, CypA, hnRNPK, RuvB2, and YB1. None of the selected proteins have so far a reported association with AAV but had a relatively high score and confidence in MS analysis. For each sample, 10 μ g of total proteins from the same samples used for MS/MS were separated using SDS/PAGE before being subjected to immunoblotting. The immunoblotting results showed that Annexin A5 (Fig. 2a), CypA, RuvB2 (Fig. 2b), and YB1 (Fig. 2c) were detected in three serotypes of purified AAV vectors, and that hnRNPK (data not shown) was not detected in any of the samples tested. Failure to detect hnRNPK in any of the vector samples may be due to the sensitivity of available antibody, as hnRNPK signal was weak even in control 293T cell lysate. Results from immunoblotting and MS study were further summarized and compared (Table 1), showing a 27% (4/15 samples tested) difference and 73% agreement in protein detection between these two different methods.

To discriminate between incorporated and copurified but unincorporated cellular proteins in AAV vectors, we used proteinase K (PK) to remove trace unincorporated cellular proteins that remained in purified vectors and were not protected by vector capsid. Figure 2c showed a comparable detection of YB1 proteins in purified AAV vectors before and after PK treatment, indicating YB1 incorporation in AAV vectors. Furthermore, there was no detection of YB1

FIG. 2. Immunoblotting analysis of cellular proteins showing the association of cellular proteins with AAV vectors before (crude) or after (pure) affinity purification (a) Annexin A5, (b) CypA and RuvB2, and (c) cellular Y-box binding protein (YB1) before proteinase K treatment and incorporated YB1 after proteinase K treatment. Control 293T, unpurified 293T cell lysate or HPLC purified parental 293T cells; PK, proteinase K; duplicate lanes, representing two independently produced and purified batches of vectors.



proteins in purified control 293T cell that had been treated and HPLC-purified in parallel with AAV vectors (lane unpurified, Fig. 2c), highlighting the specificity of the adopted AVB column for AAV vector purification and further demonstrating the incorporation of YB1 proteins in AAV vectors.

Influence of AAV production on protein expression in producer cells

In order to investigate potential influences of AAV production on the expression of both viral and cellular proteins in producer cells, we analyzed the changes in the expression of AAV capsid and Rep proteins, Annexin A5, CypA, and YB1 throughout one complete cycle of AAV production, that is, from 0 hour before the transfection of AAV and helper plasmids to 4, 6, 24 30, 48, and 72 hours after transfection when the vector production process was terminated and AAV vectors harvested. AAV capsid (VP1, VP2, and VP3) and Rep proteins could be detected 24 hours after transfection in AAV2 producer cells (Fig. 3a and b). A slight increase in the capsid protein expression in producer cells was observed from 24 to 72 h after transfection. Throughout a complete cycle of AAV production, no significant changes were observed in YB1 and CypA expression (Fig. 3c); time-dependent increase in Annexin A5 expression was observed for all three serotypes (Fig. 3d).

shRNA knockdown of Annexin A5 and YB1

Functional shRNA specifically recognizing a target gene causes down-regulation of the targeted gene expression. We

proposed that shRNA knockdown of YB1 or Annexin A5 in producer cells would impair their association with AAV virus that had been identified from the MS/MS and immunoblotting studies and would subsequently influence AAV assembly in the gene-knockdown cells. This should allow us to identify the role and importance of these genes in AAV production. For this, we used a lentiviral vector delivery system to screen 10 shRNA sequences (A1 to A5 and Y1 to Y5) targeting Annexin A5 and YB1 for their ability to down-regulate Annexin A5 and YB1, respectively. Immunoblotting analysis of gene knockdown cells shows that only the shRNA sequences A2 and A5 significantly down-regulated Annexin A5 expression (Fig. 4a); likewise, introducing Y3, Y4, or Y5 into cells resulted in significant down-regulation of YB1 (Fig. 4b) compared to controls with sequences targeting nonmammalian genes (scramble) or without a shRNA sequence (293T).

shRNA sequences A2, A5, Y4, and Y5 that showed the best gene knockdown efficiency were selected for preliminary study of their influence on AAV vector production. Our initial experiments showed that shRNA sequences A2 or A5 targeting Annexin A5 had no significant influence on the genome titers of AAV2, AAV5, and AAV8 (data not shown), and that Y5 targeting YB1 increased AAV2 titers by 2–4-fold showing significantly less influence than Y4 on AAV production; as a result, no further studies were carried using A2, A5, and Y5 shRNA sequences, and all subsequently presented results were based on the selected shRNA sequence Y4 targeting YB1 gene.

The sustainability of YB1 gene knockdown was monitored throughout the study and Fig. 4c shows sustained down-regulation of YB1 in six independent lines of YB1 knockdown cells that had been in culture for up to 80 days and had been recovered from cryo-preservation, demonstrating the sustainability of YB1 knockdown cells over time and the viability of gene knockdown cells.

Influence of YB1 gene knockdown on AAV vector production

There were a number of intrinsic practical limitations we encountered in this study; firstly there was no reporter gene,

TABLE 1. COMPARISON OF IMMUNOBLOTTING AND MASS SPECTROMETRY RESULTS

	MS			Immunoblotting		
	AAV2	AAV5	AAV8	AAV2	AAV5	AAV8
RuvB2	+	+	+	+	+	+
CypA	+	+	-	+	+	+
Annexin A5	+	+	-	+	+	+
YB1	+	+	+	+	+	+
hnRNPK	-	+	+	-	-	-

MS, mass spectrometry.

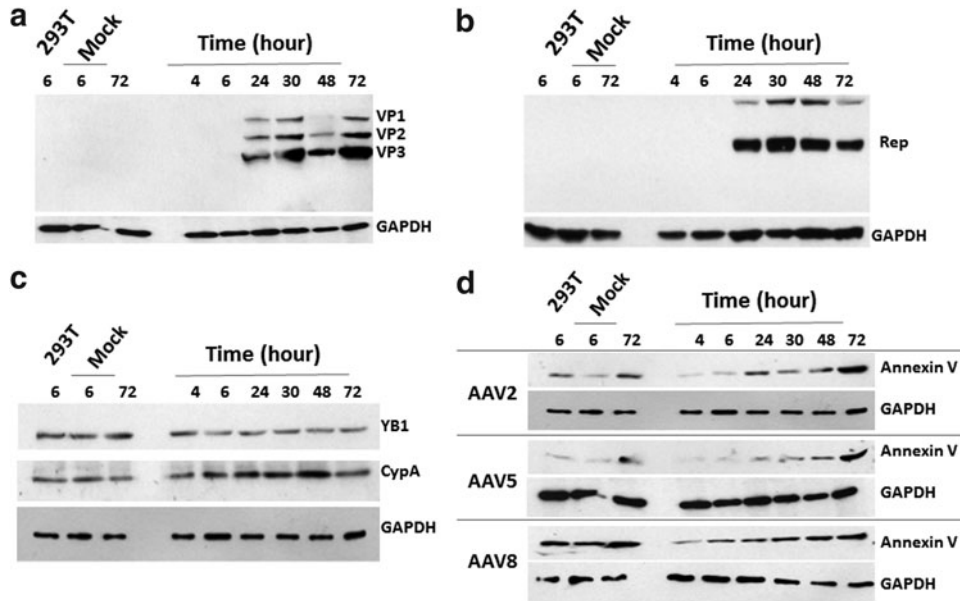


FIG. 3. Chronological analysis of protein expression using immunoblotting in parental 293T cells after transient transfection of AAV packaging and helper plasmids. (a) AAV capsids (VP1, VP2, and VP3) and (b) AAV2 Rep proteins were detected 24 h after transfection; (c) the expression of YB1 and CypA remains unchanged in AAV2 producer cells throughout a complete production cycle; and (d) increase in Annexin A5 expression was observed over time in all three serotypes of AAV. Controls: 293T cell lysate without the transfection of any plasmids (293T), 293T cells with the transfection of pcDNA3 plasmids (Mock), and housekeeping gene glyceraldehyde 3-phosphate dehydrogenase (GAPDH) as a loading control.

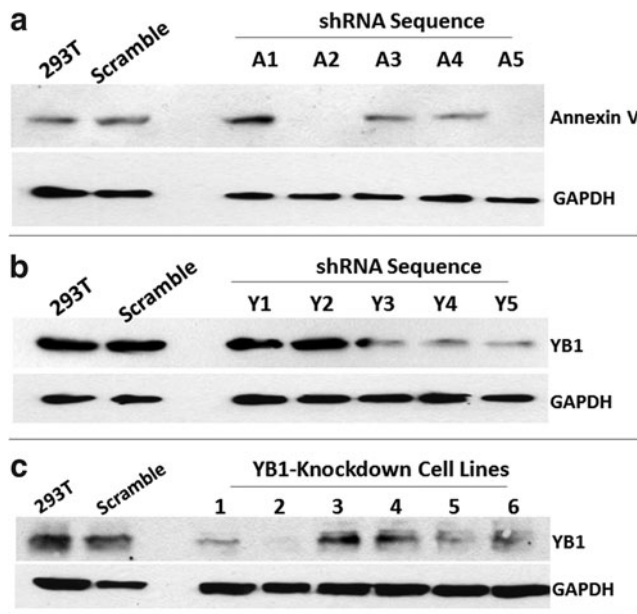
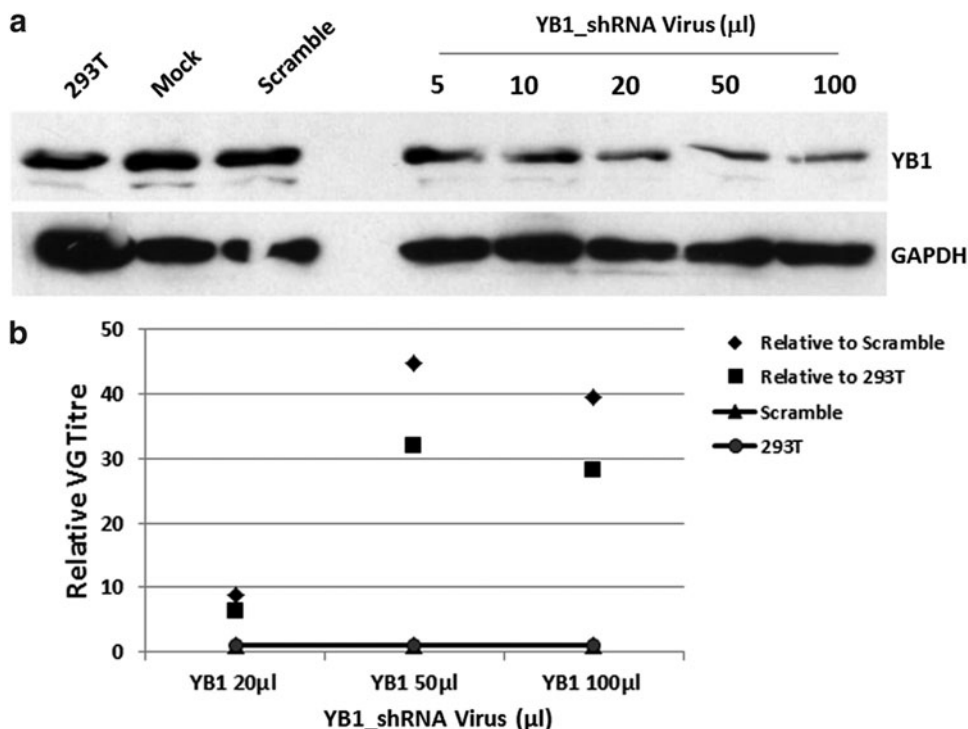


FIG. 4. Immunoblotting analysis of short hairpin RNA (shRNA) sequences targeting Annexin A5 and YB1. Significant gene knockdown was observed in the cells carrying (a) Annexin shRNA A2 or A5 sequences targeting Annexin A5 and (b) YB1 shRNA Y3, Y4, or Y5 sequences targeting YB1; (c) showing sustained down-regulation of YB1 after cryopreservation and in culture for up to 80 days in six independent lines of YB1 gene knockdown cells generated with different batches of shRNA viruses. 293T cells with a shRNA sequence targeting nonmammalian genes (scramble) and without any shRNA sequences (293T) were used as controls. Housekeeping gene GAPDH was further used as a sample loading control.

for example, GFP in the LV shRNA system for us to perform the conventional method to titrate shRNA viruses. To overcome this, we controlled and validated our gene knockdown studies for the purpose of a direct comparison by simultaneously producing all control scramble and gene-knockdown shRNA viruses under identical conditions and subsequently using an equal volume of shRNA viruses to treat the same number of cells. To optimize the amount of shRNA viruses used for YB1 gene knockdown, a serial dilution of YB1-Y4 shRNA viruses from 5 to 100 μ l per 10^5 cells were tested for gene knockdown efficiency. Figure 5a shows a slight decrease in YB1 expression in knockdown cells when increasing shRNA virus from 5 to 100 μ l, indicating a modest correlation between YB1 gene-knockdown and the amount of shRNA viruses used. The maximum effect of YB1 knockdown on vector genome titers was observed when 50 μ l of YB1-Y4 shRNA viruses were used (Fig. 5b), indicating a saturating and potential toxic effect on vector production when the amount of shRNA were further increased. As a result, all YB1 knockdown cell lines were established using 50 μ l per 10^5 cells of YB1-Y4 shRNA viruses in subsequent studies.

The second limitation in this study is the fact that YB1 knockdown cells could not survive in low cell density culture. After trying many times under different conditions including the use of parental 293T cells as a matrix to support the growth of YB1 cell clones, we failed to obtain single cell clone of YB1 knockdown cells; hence, all data presented in this study were from pooled cells. To avoid ambiguous results from the use of pooled cells, we produced and investigated seven independent lines of YB1-Y4 shRNA knockdown cells each of which using different batches of YB1-Y4 shRNA viruses. The seven lines of stable YB1

FIG. 5. Correlation of YB1 down-regulation and AAV2 production with the amount of YB1 shRNA viruses used, showing (a) a slight increase in YB1 reduction when increasing shRNA viruses and (b) relative AAV2 genome titers to control scramble and native 293T cells. The maximum effect on genome titers (VG/mL) was observed in the cells treated with 50 μ l YB1-Y4 shRNA viruses. Control samples include scramble cells with a scramble shRNA sequence (scramble) and parental 293T cells without any shRNA sequences (293T). Housekeeping gene GAPDH was used as a loading control.



knockdown cells were established by maintaining in culture for up to 100 days in the presence of 3 μ g/mL puromycin to remove the cells without puromycin-tagged shRNA. Each of the seven independent YB1 knockdown cell lines was used to produce AAV vectors in triplicates at three or more time points on around 20, 40, and 70 days after LV-shRNA transduction and at a large scale from 15 cm diameter plates containing over 10 million YB1-knockdown or control scramble cells to further minimize assay variation. Due to the scale of vector production, we had to wait 2–3 weeks for the cells to bulk up enough for one round of vector production; therefore, the time points for each cell line varied depending on the growth rate. Figure 6 shows collective data on vectors produced from seven independent cell lines over a period of 80 days. Each data point is a mean relative titer of triplicate lots of vectors produced at one time point from one line of knockdown cells. The reason for us to present collective data on the same figure from different cell lines at different time points is to show not only the relative titers but also the optimal range of production time (around 40 days) for all seven cell lines.

Introducing shRNA sequence YB1-Y4 to producer cells resulted in up to 45-fold increase in AAV2 (Fig. 6a) and 9-fold increase in AAV8 (Fig. 6b) physical vector genome titers relative to control shRNA scramble, and that the same Y4 shRNA sequence had no significant influence on AAV5 production (data not shown), indicating an intrinsic difference in response among the three serotypes of AAV. Although the reduction of YB1 expression in the knockdown cells continued for over 80 days, the maximum effect of Y4 on AAV2 production was only obtained in YB1/Y4 knockdown cells that had been in culture for 20–60 days (Fig. 6a), which may be due to a slow enrichment of YB1 knockdown cells during early puromycin selection and a lentiviral vector-associated gene silencing observed at later time points and as reported previously from other studies (Zhang *et al.*, 2010). A similar

time-dependent pattern was also observed in AAV8 producer cells (Fig. 6b).

In order to investigate whether the AAV vectors produced from YB1 knockdown cells were infectious and were able to transduce cells, AAV2 vectors were used to transduce target HeLaS3 cells. Although HeLaS3 cells contain HPV-18, no AAV replication was expected in the adopted transduction system due to the absence of *rep/cap* genes in the target cells. The number of AAV particles that were able to enter target cells was determined 16 hours after transduction by qPCR quantitation of AAV sequence copies in *actin* normalized cellular DNA, and thus designated in this study as transduction vector genome titer (TG/mL) to distinguish it from physical vector genome titers (VG/mL) that represent the packaged genome copies in a batch of AAV products. Figure 7a shows YB1 relative transduction genome titers to scramble cells; in particular, up to seven-fold increases in AAV2 transduction genome titer (TG/mL) obtained from YB1 knockdown cells compared to that from scramble cells, demonstrating the fidelity of YB1 knockdown cells in AAV production. The discrepancy, that is, up to 45- and 7-fold increases in physical vector genome titers and transduction genome titers, respectively (Fig. 6a and Fig. 7a), may be due to the limitation of the adopted transduction titrating assays.

Figure 7b shows the actual physical (hatched bars, VG/mL) and transduction (dotted bars, TG/mL) titers of AAV2 vectors produced from five independent YB1 cell lines and control scramble and 293T cells. Using CaCl₂ transient transfection, YB1 knockdown cells produced AAV2 vectors at around $\sim 10^{11}$ VG/mL per 10^8 cells; whereas parental 293T cells produced at $\sim 10^{10}$ VG/mL per 10^8 cells (hatched bars, Fig. 7b), representing a production of $\sim 10^3$ and 10^2 VG/cell in YB1 knockdown and parental 293T cells, respectively. In addition, we observed a significant difference between actual physical and transduction genome titers in

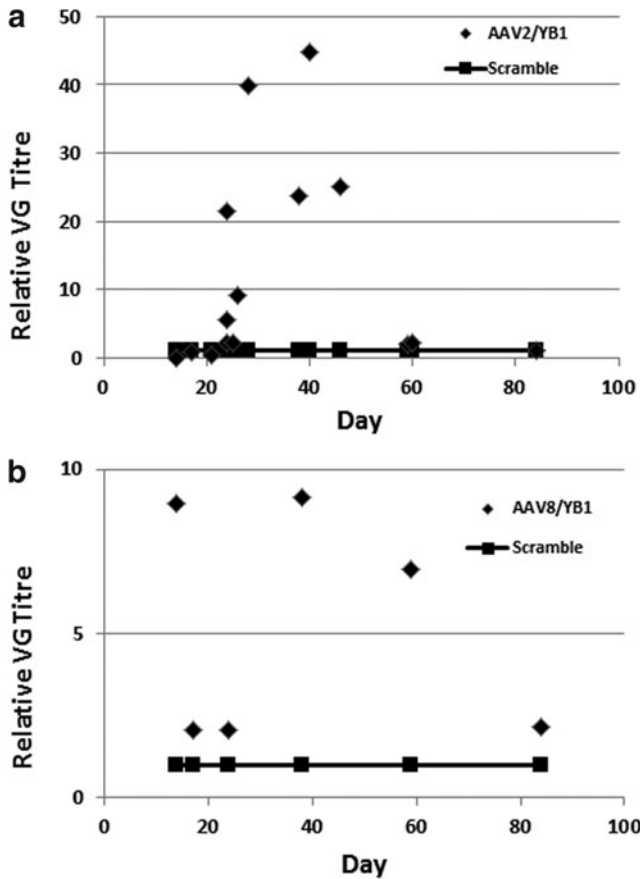


FIG. 6. Relative physical genome titers of AAV vectors produced from seven lines of YB1 gene knockdown cells to those produced from control scramble cells, showing (a) up to 45-fold increase in AAV2 vector genome titers (VG/mL) and (b) 9-fold increase in AAV8 vector genome titers (VG/mL) compared to scramble cells and throughout 80 days in culture.

the same batch of vectors. The physical genome titers (VG/mL) (hatched bars, Fig. 7b) were 2–3 logs higher than their resultant transduction genome titers (TG/mL) (dotted bars, Fig. 7b), indicating the limitation of the adopted transduction titrating assays or a potential HeLaS3 cell restriction for AAV2 transduction. A recent report has shown a significantly low transduction efficiency of AAV8 on HeLaS3 cells (Dong *et al.*, 2010); as a result, the transduction assay for AAV8 vectors was not pursued in this study.

Molecular analysis of YB1 knockdown producer cells

In order to understand the molecular mechanism of YB1 influence on AAV production, we systematically analyze AAV2 protein (Rep and Cap) expression and vector DNA production in YB1 knockdown cells. Figure 8a shows a 12- and 4-fold increase in *rep* gene expression in YB1 knockdown cells compared to that in scramble cells 24 and 72 hours after transient transfection, respectively, indicating a negative effect of native YB1 on *rep* gene expression. In contrast, the production of total AAV2 capsid proteins in YB1 knockdown cells ($1.29 \pm 0.2 \times 10^{14}$ capsids/ 10^8 cells) was ~7-fold lower than that in scramble cells ($8.87 \pm 0.1 \times 10^{14}$ capsids/ 10^8 cells) (Fig. 8b), indicating that the presence

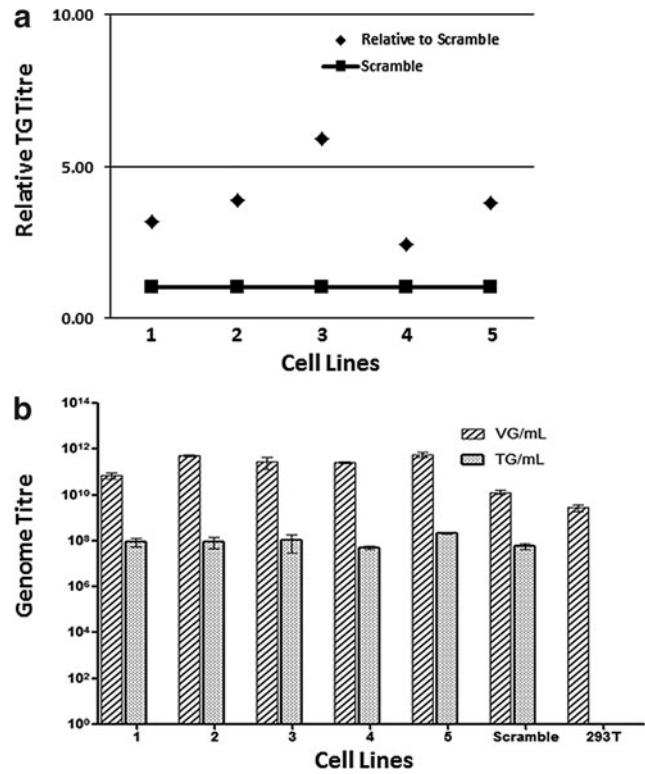


FIG. 7. Physical genome titers (VG/mL) and transduction genome titers (TG/mL) on HeLaS3 cells of vectors produced from five independent lines of YB1 knockdown (1–5), scramble, and parental 293T cells. (a) Relative transduction genome titers showing up to 7-fold increases in AAV2 vectors compared to control scramble and (b) actual physical genome titers (hatched bars, VG/mL) and transduction genome titers (dotted bars, TG/mL) of AAV2 produced from five YB1 cell lines, scramble, and parental 293T cells (n = 3).

of native YB1 was beneficial for *cap* gene expression. Furthermore, the amount of capsid proteins in the harvested vector samples was comparable between YB1 knockdown cells ($6.27 \pm 0.3 \times 10^{13}$ capsids/ 10^8 cells) and scramble ($6.77 \pm 0.2 \times 10^{13}$ capsids/ 10^8 cells) cells (Fig. 8b), indicating that vector capsid particle formation may be independent of the amount of capsid proteins produced in the cells, and that there was a limit in the number of particles to be formed in cells.

DNA integration was systematically analyzed using real-time qPCR targeting U6 sequence for YB1 shRNA integration, and targeting *rep* and CMV promoter sequences for AAV2 packaging plasmids pRep/Cap and phrGFP integration, respectively. There were $1.3 \pm 0.17 \times 10^8$ copies/ 10^8 cells of YB1 shRNA sequences detected in YB1 knockdown cells, equivalent to an average of one copy of YB1 shRNA per cell in pooled YB1 knockdown cells. Integration of AAV packaging plasmid pRep/Cap and phrGFP were comparable between scramble and YB1 knockdown cells, at $\sim 2 \times 10^7$ copies of *Rep/Cap* and $\sim 3 \times 10^7$ copies of phrGFP per 10^8 cells.

To analyze the influence of YB1 gene knockdown on the production of AAV2 vector DNA, we, using qPCR targeting vector-specific CMV sequence, systematically quantified the

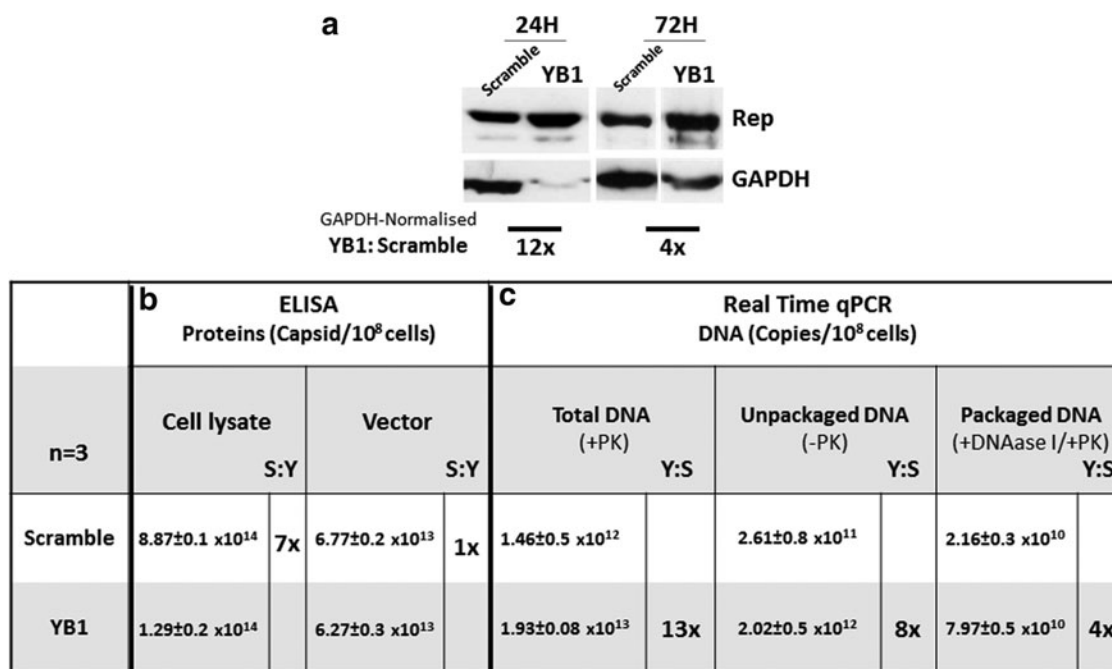


FIG. 8. Molecular analysis of YB1 knockdown cells for *rep* and *cap* expression and vector DNA production: (a) immunoblotting showing 12- and 4-fold increases in AAV2-Rep expression in YB1 knockdown cells 24 and 72 hours (H) after transient transfection, respectively; (b) ELISA showing a 7-fold decrease in *cap* expression in YB1 knockdown cell lysates compared to scramble cells and a comparable amount of Cap proteins detected in vectors harvested from YB1 and scramble cells and (c) real-time quantitative polymerase chain reaction (qPCR) showing 13× increase in total vector DNA, 8× increase in unpackaged vector DNA, and 4× increase in packaged vector DNA in YB1 knockdown cells compared to that in scramble cells. Y:S ratio between YB1 and scramble after being normalized by housekeeping gene GAPDH for immunoblotting or by cell numbers for qPCR analysis after being normalized by housekeeping gene actin. +PK, with proteinase K treatment; -PK, without proteinase K treatment; +DNAseI, with DNase I treatment; S, control scramble; Y, YB1 knockdown cells.

copies of (1) total vector DNA that contains both packaged and unpackaged vector DNA, (2) unpackaged vector DNA, and (3) packaged vector DNA in YB1 knockdown cells 72 h after transient transfection of AAV packaging plasmids. Total vector DNA was prepared by removing plasmid DNA with benzenase, removing cell membranes and nuclei after sample freeze-thawing, and disassembling AAV capsid with proteinase K to release packaged vector DNA from the capsids. It should be noted that nonintegrated vector plasmid DNA may also contribute to the total vector DNA copies in cytoplasm; however, considering the transfection and production procedure was performed in parallel and was identical for both YB1 and scramble cells, the amount of plasmid DNA in cytoplasm should likewise be comparable and would not significantly alter the calculation of *relative* total vector DNA production. Figure 8c shows that the copies of total vector DNA (+PK) were ~13-fold higher in YB1 knockdown producer cells ($1.93 \pm 0.08 \times 10^{13}$ copies/10⁸ cells) than that in scramble cells ($1.46 \pm 0.5 \times 10^{12}$ copies/10⁸ cells) indicating that YB1 gene knockdown promoted the vector DNA production.

Unpackaged AAV2 vector DNA was prepared in a similar way as that for total DNA samples except without proteinase K treatment (-PK) to release packaged vector DNA from AAV capsid. The copies of the unpackaged vector DNA were ~8× higher in YB1 knockdown cells ($2.02 \pm 0.5 \times 10^{12}$ copies/10⁸ cells) than that in scramble

cells ($2.61 \pm 0.8 \times 10^{11}$ copies/10⁸ cells) (unpackaged DNA, Fig. 8c). Packaged AAV2 vector DNA, representing physical vector genome titers, was prepared by the addition of DNase I treatment (+DNase I) to remove unpackaged vector DNA in cytoplasm followed by proteinase K treatment (+PK) to release the packaged vector DNA from capsids. The copies of packaged vector DNA (+DNase I/+PK, Fig. 8c) were 4-fold higher in YB1 knockdown cells ($7.97 \pm 0.5 \times 10^{10}$ copies/10⁸ cells) than that in scramble cells ($2.16 \pm 0.3 \times 10^{10}$ copies/10⁸ cells) (Fig. 8c). It should be noted that in this particular set of molecular studies, we observed only 4-fold increases in AAV2 vector genome titers in YB1 knockdown cells compared to that in scramble cells, which was significant but not as high as up to 45-fold as observed in early studies and as shown in Fig. 6. This may be due to the scaled down production and specific time points of the YB1 cells used in this set of studies.

In summary, the significant difference observed among the fold changes in total vector DNA (13× increase), unpackaged (8× increase), and packaged vector DNA (4× increase) underlined a potential for the improvement of AAV vector DNA packaging in YB1 production system. Moreover, taking into consideration that the amount of capsid proteins was comparable (Fig. 8b) but the copies of packaged DNA (Fig. 8c) was 4-fold higher in the same batch of harvested vector samples from YB1 knockdown cells compared to that from scramble cells, our results revealed

a considerable advantage of YB1 gene knockdown in reducing the number of empty particles in AAV products.

Discussion

This study revealed for the first time an important role of Y-box binding protein 1 (YB1) in AAV vector production. Introducing the shRNA sequence Y4 that targets and down-regulates the YB1 gene to AAV producer cells resulted in up to 45- and 9-fold increase in physical genome titers of AAV2 and AAV8, respectively, and up to 7-fold increase in AAV2 infectious genome titers. Molecular characterization of YB1 knockdown cells showed an ~12-fold increase in *rep* expression, an ~13-fold increase in vector DNA production, and an ~7-fold decrease in *cap* expression in YB1 knockdown cells compared to scramble cells, uncovering a significant role of the YB1 gene in AAV biology.

Our results show a serotype-specific role of YB1 in AAV production; in particular, knockdown of YB1 improved AAV2 and AAV8 production by 45- and 9-fold, respectively, but had no significant effect on AAV5 production. The three serotypes of AAV vectors investigated in this study have identical *rep* and ITR sequences and were produced in the presence of the same helper elements from adenoviruses. In terms of differences among the three serotypes of AAV2, AAV5, and AAV8 vectors, the serotype-specific *cap* gene sequences are clearly one of them. AAV2 and AAV8 capsid proteins share more than 82% homology in their primary sequence and a much similar overall topology in the structure of capsid proteins (Kerr *et al.*, 2006). The notable structural differences between AAV2 and AAV8 capsid proteins are located on the capsid surface and are known to be associated with the binding property of AAV2 and AAV8 to target cells rather than being involved in capsid assembly and genome packaging (Nam *et al.*, 2007), further demonstrating the similarity between AAV2 and AAV8 in terms of capsid assembly. In contrast, AAV5 is one of the most divergent AAV serotypes, sharing only ~55% sequence homology to other serotypes, including AAV2 and AAV8. Unique structural features of AAV5 capsid proteins, including a smaller HI and VR-IV loop and larger VR-VII, are located in the VP region that controls the specificity of capsid assembly, genome packaging, and antigenic determinants (Govindasamy *et al.*, 2013), and may explain the difference in AAV2 and AAV8 vector production that we observed. Our results also show that YB1 gene knockdown resulted in up to 12- and 13-fold increases in *rep* gene expression and vector DNA production, respectively, and an ~7-fold decrease in *cap* gene expression, underlying the molecular mechanism of YB1 influence on AAV vector production.

YB1 is a DNA and RNA-binding protein involved in almost all DNA and mRNA-dependent processes. YB1 packs and stabilizes mRNA to mediate gene regulation at different levels (Eliseeva *et al.*, 2011). YB1 has a far higher affinity for a single-stranded DNA (ssDNA) than double-stranded DNA (Hasegawa *et al.*, 1991; MacDonald *et al.*, 1995; Izumi *et al.*, 2001; Coles *et al.*, 2005) and has the greatest binding preference for the single-stranded DNA motif GGGG(TT) (Zasedateleva *et al.*, 2002). Analysis of the single-stranded AAV2 DNA genome showed that such a single-stranded GGGG(TT) motif is presented within the

AAV2 ITR region from nucleotide 137 to 142 of the AAV2 genome (NCBI sequence NC_001401.2), indicating a potential AAV DNA binding site for the YB1 protein. ITR deletion mutagenesis showed that the 20 nucleotide D sequence (from nucleotide 126–146), which covers the single-stranded GGGG(TT) motif and immediately follows the 125 nucleotide long hairpin, is required for the encapsidation of the AAV DNA genome and has thus been proposed as packaging signal for AAV; in particular, the N-terminal region of AAV capsid proteins binds to the D sequence resulting in the encapsidation of AAV ssDNA into pre-assembled AAV capsid (Wang *et al.*, 1996; Wang and Srivastava, 1997; Xiao *et al.*, 1997). Therefore, the capability of both YB1 and AAV capsids for binding to the ITR D sequence region may impose competition between YB1 and AAV capsids and compromise encapsidation of AAV genome.

There are three YB1 domains, that is, A/P, CSD, and CTD, involved in protein–protein interactions (Eliseeva *et al.*, 2011). In particular, YB1 plays an important role in the replication of a number of viruses via binding to viral proteins, for example, HIV TAT (Ansari *et al.*, 1999), HIV Rev (Kramer-Hämmerle *et al.*, 2005), large T antigen of polyomavirus (Safak *et al.*, 2002), Hepatitis C virus (HCV) protein NS3/4A (Chatel-Chaix *et al.*, 2011), and influenza viral ribonucleoprotein (RNP) (Kawaguchi *et al.*, 2012). Using an shRNA gene knockdown approach similar to ours, Chatel-Chaix *et al.* (2011, 2013) reported that down-regulation of YB1 resulted in the reduction of HCV infectious titer by up to 80%; however, down-regulation of YB1 did not influence the expression of viral proteins and the production and stability of vRNA, indicating that knockdown YB1 disrupted the formation of a YB1-NS3/4A-vRNA interactome required for recruiting core proteins for virus assembly.

Studying the role of YB1 in adenovirus replication is particularly relevant to the understanding of our findings that down-regulation of YB1 significantly improved AAV production by as much as 45-fold. It has been previously reported that in adenovirus-infected cells, the interaction of adenoviral protein E1B with YB1 resulted in the accumulation of YB1 in nuclei, YB1 activation of the E2A gene (Holm *et al.*, 2002), and subsequently the initiation of adenoviral DNA replication (Holm *et al.*, 2002; Glockzin *et al.*, 2006). Overexpression of YB1-regulated adenoviral E2 promoter in an E1-independent manner led not only to adenoviral DNA replication but also a 2–3-log increase in the production of infectious particles from E1-deleted adenovirus vectors (Holm *et al.*, 2002; Glockzin *et al.*, 2006). As a result, overexpression of YB1 has been further exploited in adenovirus-based vector development and virotherapy (Glockzin *et al.*, 2006; Rognoni *et al.*, 2009).

So far there has been no direct association of YB1 reported with AAV virus; however, the role of adenovirus in the AAV life cycle has been well documented, and this may facilitate understanding the mechanism behind the enhancement of YB1 knockdown on AAV vector production. The AAV production system used in our study provided four adenoviral elements, that is, E1, E2A, E4, and VA genes that were expressed either stably in the producer cells or transiently from a plasmid with helper function for AAV. Open-reading frame 6 of the E4 region is important for the

conversion of the single-stranded AAV genome into a double-stranded form, which is the substrate for subsequent steps in DNA replication (Ferrari *et al.*, 1996; Fisher *et al.*, 1996). Protein E2A plays a key role in viral DNA replication via binding to AAV viral DNA, promoting DNA elongation (Klessig and Grodzicker, 1979; Chang and Shenk, 1990), and displacement of the elongating strand from its template (Ward *et al.*, 1998). Both YB1 and E2A are DNA binding proteins (DBP) but differ from each other in their cellular and viral origins, respectively. YB1 and E2A share a comparable binding preference for single-stranded DNA. It is possible that adenoviral E2A has a prime regulation property for cellular DNA binding proteins (cellular DBP) in the AAV life cycle; therefore, down-regulation of YB1 would reduce the competition of YB1 binding to AAV DNA, resulting in the enhancement of E2A-AAV DNA interaction, the efficiency of AAV DNA replication, and ultimately an increase in AAV vector genome titers. This hypothesis is supported by the observation that cells lacking AAV helper components including E2A could still produce small amounts of AAV particles, indicating a low level of cellular helper function from abundant but less efficient cellular DBPs, for example, YB1 in the AAV life cycle (Yalkinoglu *et al.*, 1988).

On the other hand, adenoviral proteins E1A-E1B and E2A play an important role in activating AAV2 p5 promoter (Chang *et al.*, 1989), resulting in the transcription and expression of the AAV2 *rep* gene. There have been a significant number of reports on the mechanism of YB1 regulation of cellular and viral promoters. Coles *et al.* (2005) demonstrated that binding of YB1 to the vascular endothelial growth factor promoter prevented the binding of other transcription factors and resulted in the inhibition of transcription and translation. It has also been shown that YB1 binding to the ssDNA region of a promoter resulted in the stabilization of ssDNA that also inhibited gene transcription and translation (Zasedateleva *et al.*, 2002; Dooley *et al.*, 2006). Therefore, it is possible that down-regulation of YB1 promoted E2A binding to the AAV2p5 promoter that synergistically contributed to the significant increase in AAV Rep gene expression and vector titers observed in this study.

Taking into account the potential roles of YB1 in DNA replication, ssDNA binding, and AAV transcription and translation, our results support that down-regulation of YB1 results not only in increase in *rep* gene expression under the control of the AAV2p5 promoter but also an increase in AAV DNA production and ssDNA encapsidation via reducing YB1 competition with E2A and AAV capsids for AAV2 ssDNA, in particular the AAV2 ITR sequence. In addition, the native AAV2p5 promoter in AAV2/2 vectors may perform more effectively compared to the chimeric AAV2/8 Rep/Cap in the expression of Rep proteins and cause the observed difference in fold changes noted, that is, 45- and 9-fold increase in AAV2 and AAV8 production, respectively. In the case of AAV5 vectors, vector DNA replication may likewise be increased via a similar competition-based mechanism as for AAV2 and AAV8; however, the distinctive AAV5 capsid proteins may be less dependent on combined YB1 and adenoviral helper function. The potential interaction and competition of YB1, E2A, and AAV capsid proteins with AAV genome are currently under investigation.

In summary, a novel YB1 knockdown cell line has been established, demonstrating a significant enhancement in AAV production with up to 45- and 9-fold increase in physical genome titers of AAV2 and AAV8, respectively, and up to a 7-fold increase in AAV2 transduction/infectious genome titers. The significant increase in AAV2 vector titers may be due to a significant increase in *rep* gene expression (up to 12-fold) and vector DNA production (up to 13-fold) in YB1 knockdown cells compared to scramble cells. Our results also demonstrated a significant reduction in the numbers of empty particles presented in AAV2 vector products. Although there has been, so far, no direct involvement of YB1 in the AAV life cycle reported, it is speculated that YB1 exerts negative effects on AAV production via YB1 competition with E2A and AAV capsid proteins for binding to the ITR sequence and AAV2p5 promoter, thus impairing AAV *rep* gene expression, vector DNA replication, and ssDNA encapsidation. The precise mechanism of YB1 effects in AAV production requires further investigation. Understanding the role of YB1 in the AAV life cycle greatly facilitates future production of high titer AAV vectors and, ultimately, improves the quality and safety of AAV vectors for clinical use.

Acknowledgments

The project is funded by the UK Department of Health. The authors would like to thank Natalie Werling for her technical support.

Author Disclosure Statement

No competing financial interests exist for all authors.

References

- Ansari, S.A., Safak, M., Gallia, G.L., *et al.* (1999). Interaction of YB-1 with human immunodeficiency virus type 1 Tat and TAR RNA modulates viral promoter activity. *J Gen Virol* 80 (Pt 10), 2629–2638.
- Bennett, J., Ashtari, M., Wellman, J., *et al.* (2012). AAV2 gene therapy readministration in three adults with congenital blindness. *Sci Transl Med* 4, 120ra15.
- Bevington, J.M., Needham, P.G., Verrill, K.C., *et al.* (2007). Adeno-associated virus interactions with B23/Nucleophosmin: identification of sub-nucleolar virion regions. *Virology* 357, 102–113.
- Bleker, S., Pawlita, M., and Kleinschmidt, J.A. (2006). Impact of capsid conformation and Rep-capsid interactions on adeno-associated virus type 2 genome packaging. *J Virol* 80, 810–820.
- Brument, N., Morenweiser, R., Blouin, V., *et al.* (2002). A versatile and scalable two-step ion-exchange chromatography process for the purification of recombinant adeno-associated virus serotypes-2 and -5. *Mol Ther* 6, 678–686.
- Bryant, L.M., Christopher, D.M., Giles, A.R., *et al.* (2013). Lessons learned from the clinical development and market authorization of Glybera. *Hum Gene Ther Clin Dev* 24, 55–64.
- Carter, B.J. (2004) Adeno-associated virus helper functions. In *Handbook of Parvoviruses*, Vol. 1. P. Tijssen, ed. (CRC Press, Boca Raton, FL), pp. 255–295.
- Chang, L.S., and Shenk, T. (1990). The adenovirus DNA-binding protein stimulates the rate of transcription directed by adenovirus and adeno-associated virus promoters. *J Virol* 64, 2103–2109.

- Chang, L.S., Shi, Y., and Shenk, T. (1989). Adeno-associated virus P5 promoter contains an adenovirus E1A-inducible element and a binding site for the major late transcription factor. *J Virol* 63, 3479–3488.
- Chatel-Chaix, L., Melançon, P., Racine, M., *et al.* (2011). Y-box-binding protein 1 interacts with hepatitis C virus NS3/4A and influences the equilibrium between viral RNA replication and infectious particle production. *J Virol* 85, 11022–11037.
- Chatel-Chaix, L., Germain, M.A., Motorina, A., *et al.* (2013). A host YB-1 ribonucleoprotein complex is hijacked by hepatitis C virus for the control of NS3-dependent particle production. *J Virol* 87, 11704–11720.
- Chen, C.A., and Okayama, H. (1988). Calcium phosphate-mediated gene transfer: a highly efficient transfection system for stably transforming cells with plasmid DNA. *Biotechniques* 6, 632–638.
- Coles, L.S., Lambrusco, L., Burrows, J., *et al.* (2005). Phosphorylation of cold shock domain/Y-box proteins by ERK2 and GSK3beta and repression of the human VEGF promoter. *FEBS Lett* 579, 5372–5378.
- Davidoff, A.M., Ng, C.Y., Sleep, S., *et al.* (2004). Purification of recombinant adeno-associated virus type 8 vectors by ion exchange chromatography generates clinical grade vector stock. *J Virol Methods* 121, 209–215.
- Denard, J., Rundwasser, S., Laroudie, N., *et al.* 2009. Quantitative proteomic analysis of lentiviral vectors using 2-DE. *Proteomics* 9, 3666–3676.
- DiPrimio, N., Asokan, A., Govindasamy, L., *et al.* (2008). Surface loop dynamics in adeno-associated virus capsid assembly. *J Virol* 82, 5178–5189.
- Dong, X., Tian W., Wang G., *et al.* (2010). Establishment of an AAV reverse infection-based array. *PLoS One* 5, e13479.
- Dong, B., Duan, X., Chow, H.Y., *et al.* (2014). Proteomics analysis of co-purifying cellular proteins associated with rAAV vectors. *PLoS One* 9, e86453.
- Dooley, S., Said, H.M., Gressner, A.M., *et al.* (2006). Y-box protein-1 is the crucial mediator of antifibrotic interferon-gamma effects. *J Biol Chem* 281, 1784–1795.
- Eliseeva, I.A., Kim, E.R., Guryanov, S.G., *et al.* (2011). Y-box-binding protein 1 (YB-1) and its functions. *Biochemistry (Mosc)* 76, 1402–1433.
- Ferrari, F.K., Samulski, T., Shenk, T., and Samulski, R.J. (1996). Second-strand synthesis is a rate-limiting step for efficient transduction by recombinant adeno-associated virus vectors. *J Virol* 70, 3227–3234.
- Fisher, K.J., Gao, G.P., Weitzman, M.D., *et al.* (1996). Transduction with recombinant adeno-associated virus for gene therapy is limited by leading-strand synthesis. *J Virol* 70, 520–532.
- Gao, G.P., Qu, G., Faust, L.Z., *et al.* (1998). High-titer adeno-associated viral vectors from a Rep/Cap cell line and hybrid shuttle virus. *Hum Gene Ther* 9, 2353–2562.
- Gerlach, B., Kleinschmidt, J.A., and Böttcher, B. (2011). Conformational changes in adeno-associated virus type 1 induced by genome packaging. *J Mol Biol* 409, 427–438.
- Glockzin, G., Mantwill, K., Jurchott, K., *et al.* (2006). Characterization of the recombinant adenovirus vector AdYB-1: implications for oncolytic vector development. *J Virol* 80, 3904–3911.
- Govindasamy, L., Dimattia, M.A., Gurda, B.L., *et al.* (2013). Structural insights into adeno-associated virus serotype 5. *J Virol* 87, 11187–11199.
- Hasegawa, S.L., Doetsch, P.W., Hamilton, K.K., *et al.* (1991). DNA binding properties of YB-1 and dbpA: binding to double-stranded, single-stranded, and abasic site containing DNAs. *Nucleic Acids Res* 19, 4915–4920.
- Holm, P.S., Bergmann, S., Jurchott, K., *et al.* (2002). YB-1 relocates to the nucleus in adenovirus-infected cells and facilitates viral replication by inducing E2 gene expression through the E2 late promoter. *J Biol Chem* 277, 10427–10434.
- Izumi, H., Imamura, T., Nagatani, G., *et al.* (2001). Y box-binding protein-1 binds preferentially to single-stranded nucleic acids and exhibits 3'→5' exonuclease activity. *Nucleic Acids Res* 29, 1200–1207.
- Jessup, M., Greenberg, B., Mancini, D., *et al.* (2011). Calcium Upregulation by Percutaneous Administration of Gene Therapy in Cardiac Disease (CUPID): a phase 2 trial of intracoronary gene therapy of sarcoplasmic reticulum Ca²⁺-ATPase in patients with advanced heart failure. *Circulation* 124, 304–313.
- Johnson, J.S., and Samulski, R.J. (2009). Enhancement of adeno-associated virus infection by mobilizing capsids into and out of the nucleolus. *J Virol* 83, 2632–2644.
- Kaludov, N., Handelman, B., and Chiorini, J.A. (2002). Scalable purification of adeno-associated virus type 2, 4, or 5 using ion-exchange chromatography. *Hum Gene Ther* 13, 1235–1243.
- Kawaguchi, A., Matsumoto, K., and Nagata, K. (2012). YB-1 functions as a porter to lead influenza virus ribonucleoprotein complexes to microtubules. *J Virol* 86, 11086–11095.
- Kerr, J.R., Cotmore, S.F., Bloom, M.E., *et al.* (2006) *Parvoviruses*. (Hodder Arnold Publisher, London) pp. 305–319.
- King, J.A., Dubielzig, R., Grimm, D., and Kleinschmidt, J. A. (2001). DNA helicase-mediated packaging of adeno-associated virus type 2 genomes into preformed capsids. *EMBO J* 20, 3282–3291.
- Klessig, D.F., and Grodzicker, T. (1979). Mutations that allow human Ad2 and Ad5 to express late genes in monkey cells map in the viral gene encoding the 72K DNA binding protein. *Cell* 17, 957–966.
- Kramer-Hämmerle, S., Ceccherini-Silberstein, F., Bickel, C., *et al.* (2005). Identification of a novel Rev-interacting cellular protein. *BMC Cell Biol* 6, 20.
- Lock, M., Alvira, M.R., and Wilson, J.M. (2012). Analysis of particle content of recombinant adeno-associated virus serotype 8 vectors by ion-exchange chromatography. *Hum Gene Ther Methods* 23, 56–64.
- MacDonald, G.H., Itoh-Lindstrom, Y., and Ting, J.P. (1995). The transcriptional regulatory protein, YB-1, promotes single-stranded regions in the DRA promoter. *J Biol Chem* 270, 3527–3533.
- Martin, J., Frederick, A., Luo, Y., *et al.* (2013). Generation and characterization of adeno-associated virus producer cell lines for research and preclinical vector production. *Hum Gene Ther Methods* 24, 253–269.
- Muzyczka, N. (1992). Use of adeno-associated virus as a general transduction vector for mammalian cells. *Curr Top Microbiol Immunol* 158, 97–129.
- Myers, M.W., and Carter, B.J. (1980). Assembly of adeno-associated virus. *Virology* 102, 71–82.
- Nam, H.J., Lane, M.D., Padron, E., *et al.* (2007). Structure of adeno-associated virus serotype 8, a gene therapy vector. *J Virol* 81, 12260–12271.
- Nathwani, A.C., Tuddenham, E.G., Rangarajan, S., *et al.* (2011). Adenovirus-associated virus vector-mediated gene transfer in hemophilia B. *N Engl J Med* 365, 2357–2365.
- Naumer, M., Sonntag, F., Schmidt, K., *et al.* (2012). Properties of the adeno-associated virus assembly-activating protein. *J Virol* 86, 13038–13048.

- Nicolas, A., Jolinon, N., Alazard-Dany, N., *et al.* (2012). Factors influencing helper-independent adeno-associated virus replication. *Virology* 432, 1–9.
- Okada, T., Nonaka-Sarukawa, M., Uchibori, R., *et al.* (2009). Scalable purification of adeno-associated virus serotype 1 (AAV1) and AAV8 vectors, using dual ion-exchange adsorptive membranes. *Hum Gene Ther* 20, 1013–1021.
- Qiu, J., and Brown, K.E. (1999). A 110-kDa nuclear shuttle protein, nucleolin, specifically binds to adeno-associated virus type 2 (AAV-2) capsid. *Virology* 257, 373–382.
- Qu, G., Bahr-Davidson, J., Prado, J., *et al.* (2007). Separation of adeno-associated virus type 2 empty particles from genome containing vectors by anion-exchange column chromatography. *J Virol Methods* 140, 183–192.
- Rognoni, E., Widmaier, M., Haczek, C., *et al.* (2009). Adenovirus-based virotherapy enabled by cellular YB-1 expression in vitro and in vivo. *Cancer Gene Ther* 16, 753–763.
- Safak, M., Sadowska, B., Barrucco, R., and Khalili, K. (2002). Functional interaction between JC virus late regulatory agnoprotein and cellular Y-box binding transcription factor, YB-1. *J Virol* 76, 3828–3838.
- Shiau, A.L., Liu, P.S., and Wu, C.L. (2005). Novel strategy for generation and titration of recombinant adeno-associated virus vectors. *J Virol* 79, 193–201.
- Sonntag, F., Köther, K., Schmidt, K., *et al.* (2011). The assembly-activating protein promotes capsid assembly of different adeno-associated virus serotypes. *J Virol* 85, 12686–12697.
- Steinbach, S., Wistuba, A., Bock, T., and Kleinschmidt, J.A. (1997). Assembly of adeno-associated virus type 2 capsids in vitro. *J Gen Virol* 78 (Pt 6), 1453–14562.
- Wang, X.S., and Srivastava, A. (1997). A novel terminal resolution-like site in the adeno-associated virus type 2 genome. *J Virol* 71, 1140–1146.
- Wang, X.S., Ponnazhagan, S., and Srivastava, A. (1996). Rescue and replication of adeno-associated virus type 2 as well as vector DNA sequences from recombinant plasmids containing deletions in the viral inverted terminal repeats: selective encapsidation of viral genomes in progeny virions. *J Virol* 70, 1668–1677.
- Ward, P., Dean, F.B., O'Donnell, M.E., and Berns, K.I. (1998). Role of the adenovirus DNA-binding protein in in vitro adeno-associated virus DNA replication. *J Virol* 72, 420–427.
- Wu, X. (2001). A novel method for purification of recombinant adeno-associated virus vectors on a large scale. *Chin Sci Bull* 46, 485–489.
- Xiao, X., Xiao, W., Li, J., and Samulski, R.J. (1997). A novel 165-base-pair terminal repeat sequence is the sole cis requirement for the adeno-associated virus life cycle. *J Virol* 71, 941–948.
- Yalkinoglu, A.O., Heilbronn, R., Bürkle, A., *et al.* (1988). DNA amplification of adeno-associated virus as a response to cellular genotoxic stress. *Cancer Res* 48, 3123–3129.
- Zasedateleva, O.A., Krylov, A.S., Prokopenko, D.V., *et al.* (2002). Specificity of mammalian Y-box binding protein p50 in interaction with ss and ds DNA analyzed with generic oligonucleotide microchip. *J Mol Biol* 324, 73–87.
- Zhang, F., Frost, A.R., Blundell, M.P., *et al.* (2010). A ubiquitous chromatin opening element (UCOE) confers resistance to DNA methylation-mediated silencing of lentiviral vectors. *Mol Ther* 18, 1640–1649.

Address correspondence to:

Yuan Zhao

Division of Advance Therapies

National Institute for Biological Standards and Control

Medicines and Health Products Regulatory Agency

Blanche Lane

South Mimms

Hertfordshire EN6 3QG

United Kingdom

E-mail: yuan.zhao@nibsc.org

Received for publication April 10, 2014;

accepted after revision July 21, 2014.

Published online: July 29, 2014.

Supplementary Data

SUPPLEMENTARY TABLE S1. LIST OF PROTEINS IDENTIFIED IN LIQUID CHROMATOGRAPHY-MASS SPECTROMETRY/MASS SPECTROMETRY STUDIES

	<i>Protein ID</i>	AAV2	AAV5	AAV8	
Shared by 3 serotypes (10 proteins)	Glyceraldehyde-3-phosphate dehydrogenase (fragment) OS=Homo sapiens GN=GAPD PE=2 SV=1 - [Q5ZEY3_HUMAN]	+	+	+	
	Heat shock 70kDa protein 1A/1B OS=Homo sapiens GN=HSPA1A PE=1 SV=5 - [HSP71_HUMAN]	+	+	+	
	Histone H2A type 1-H OS=Homo sapiens GN=HIST1H2AH PE=1 SV=3 - [H2A1H_HUMAN]	+	+	+	
	Histone H2B OS=Homo sapiens PE=2 SV=1 - [A8K9J7_HUMAN]	+	+	+	
	60S acidic ribosomal protein P2 OS=Homo sapiens GN=RPLP2 PE=1 SV=1 - [RLA2_HUMAN]	+	+	+	
	Alpha-enolase OS=Homo sapiens GN=ENO1 PE=1 SV=2 - [ENOA_HUMAN]	+	+	+	
	Nucleolin, isoform CRA_c OS=Homo sapiens GN=NCL PE=2 SV=1 - [B3KM80_HUMAN]	+	+	+	
	Nucleophosmin OS=Homo sapiens GN=NPM1 PE=1 SV=2 - [NPM_HUMAN]	+	+	+	
	YBX1 protein (Fragment) OS=Homo sapiens GN=YBX1 PE=2 SV=1 - [Q6PKI6_HUMAN]	+	+	+	
	RuvB-like 2 OS=Homo sapiens GN=RUVBL2 PE=1 SV=3 - [RUVB2_HUMAN]	+	+	+	
	Shared by 2 serotypes (8 proteins)	Annexin A5 OS=Homo sapiens GN=ANXA5 PE=1 SV=2 - [ANXA5_HUMAN]	+	+	
		Brain acid soluble protein 1 OS=Homo sapiens GN=BASP1 PE=1 SV=2 - [BASP1_HUMAN]	+	+	
		Histone H2A.x OS=Homo sapiens GN=H2AFX PE=1 SV=2 - [H2AX_HUMAN]	+		+
		MARCKS protein (Fragment) OS=Homo sapiens GN=MARCKS PE=2 SV=1 - [Q6NV11_HUMAN]	+	+	
MYL6 protein OS=Homo sapiens GN=MYL6 PE=2 SV=1 - [Q6IBG5_HUMAN]		+	+		
Nascent polypeptide-associated complex alpha subunit (CypA) (Fragment) OS=Homo sapiens GN=NACA PE=4 SV=1 - [F8W1N5_HUMAN]		+	+		
Heterogeneous nuclear ribonucleoprotein K (hnRNPK) OS=Homo sapiens GN=HNRNPK PE=2 SV=1 - [Q5T6W5_HUMAN]			+	+	
Peptidyl-prolyl cis-trans isomerase (Fragment) OS=Homo sapiens GN=PPIH PE=3 SV=1 - [C9JQD4_HUMAN]		+		+	
Unique to 1 serotype (26 proteins)	Putative uncharacterized protein (Fragment) OS=Homo sapiens PE=2 SV=1 - [Q8WVW5_HUMAN]			+	
	RuvB-like 1 (Fragment) OS=Homo sapiens GN=RUVBL1 PE=2 SV=1 - [B5BUB1_HUMAN]	+			
	Triosephosphate isomerase (Fragment) OS=Homo sapiens PE=2 SV=1 - [Q53HE2_HUMAN]	+			
	78 kDa glucose-regulated protein OS=Homo sapiens GN=HSPA5 PE=1 SV=2 - [GRP78_HUMAN]		+		
	ATP synthase subunit beta (Fragment) OS=Homo sapiens GN=ATP5B PE=2 SV=1 - [Q0QEN7_HUMAN]		+		
	Chaperonin 10-related protein (Fragment) OS=Homo sapiens GN=EPFP1 PE=2 SV=1 - [Q9UNM1_HUMAN]		+		
	L-lactate dehydrogenase B chain OS=Homo sapiens GN=LDHB PE=1 SV=2 - [LDHB_HUMAN]	+			
	Synaptic vesicle membrane protein VAT-1 homolog OS=Homo sapiens GN=VAT1 PE=1 SV=2 - [VAT1_HUMAN]	+			

(continued)

SUPPLEMENTARY TABLE S1. (CONTINUED)

<i>Protein ID</i>	AAV2	AAV5	AAV8
Actin, gamma 1 OS=Homo sapiens GN=ACTG1 PE=3 SV=1 - [F5H0N0_HUMAN]		+	
Annexin A2 (Fragment) OS=Homo sapiens GN=ANXA2 PE=4 SV=1 - [H0YKZ7_HUMAN]		+	
ATP synthase subunit alpha OS=Homo sapiens PE=2 SV=1 - [B4DY56_HUMAN]		+	
ATP synthase-coupling factor 6, mitochondrial OS=Homo sapiens GN=ATP5J PE=1 SV=1 - [ATP5J_HUMAN]		+	
Capsid protein VP1 OS=Adeno-associated virus 2 (isolate Srivastava/1982) PE=1 SV=2 - [CAPSD_AAV2S]	+		
Capsid protein OS=Adeno-associated virus - 5 GN=cap PE=1 SV=1 - [Q9YIJ1_9VIRU]		+	
Capsid protein OS=Adeno-associated virus - 8 PE=1 SV=1 - [Q8JQF8_9VIRU]			+
Cofilin 1 (non-muscle) (Fragment) OS=Homo sapiens GN=CFL1 PE=4 SV=1 - [E9PLJ3_HUMAN]		+	
Complement component 1 Q subcomponent-binding protein, mitochondrial OS=Homo sapiens GN=C1QBP PE=1 SV=1 - [C1QBP_HUMAN]		+	
Erythrocyte membrane protein band 4.1-like 3 OS=Homo sapiens GN=EPB41L3 PE=2 SV=1 - [A8K968_HUMAN]		+	
Heterogeneous nuclear ribonucleoprotein A1 (Fragment) OS=Homo sapiens GN=HNRNPA1 PE=4 SV=1 - [F8VTQ5_HUMAN]			+
Myosin-10 OS=Homo sapiens GN=MYH10 PE=1 SV=3 - [MYH10_HUMAN]		+	
Myosin-9 OS=Homo sapiens GN=MYH9 PE=1 SV=4 - [MYH9_HUMAN]		+	
Serine/arginine repetitive matrix protein 1 OS=Homo sapiens GN=SRRM1 PE=1 SV=2 - [SRRM1_HUMAN]	+		
Single-stranded DNA binding protein 1 (Fragment) OS=Homo sapiens GN=SSBP1 PE=4 SV=1 - [C9K0U8_HUMAN]			+
Uncharacterized protein OS=Homo sapiens GN=SLC1A5 PE=2 SV=1 - [B4DWS4_HUMAN]		+	
Methylenetetrahydrofolate dehydrogenase (NADP+ dependent) 1, methenyltetrahydrofolate cyclohydrolase, formyltetrahydrofolate synthetase OS=Homo sapiens GN=MTHFD1 PE=3 SV=1 - [G3V2B8_HUMAN]		+	
Nucleolar RNA helicase 2 OS=Homo sapiens GN=DDX21 PE=1 SV=5 - [DDX21_HUMAN]		+	